Use of elastoplasticity to simulate cyclic sand behavior

A. G. Papadimitriou & G. D. Bouckovalas
National Technical University of Athens Greece

Y. F. Dafalias
National Technical University of Athens Greece and University of California at Davis USA

ABSTRACT: The presented elastoplastic model for sands combines a Ramberg-Osgood non-linear hysteretic formulation at small and intermediate cyclic shear strains ($< 10^{-2}$ %) and a bounding surface plasticity formulation at larger strains. The emphasis is on the explicit use of the State Parameter and on the effect of fabric evolution during monotonic and cyclic loading. Comparison with experiments shows that it is possible to predict quantitatively all basic aspects of cyclic behavior, using the same set of density independent model parameters. Namely: a) the degradation of shear modulus and the concurrent increase of hysteretic damping ratio with cyclic shear strain, b) the rates of plastic shear strain and excess pore pressure accumulation with number of cycles, and c) the resistance to liquefaction.

1 INTRODUCTION

Current state of practice in elastoplastic modelling of sand behavior has finally addressed the issue of predicting the effect of density in monotonic loading with a single set of model parameters. This task has been proven difficult for models that were founded on the framework of Critical State Soil Mechanics (Roscoe et al. 1958, Schofield & Wroth 1968). Two key alterations to this framework had to be introduced: a) allowance for the experimentally established infinity of normal consolidation lines before crushing of sand particles, as opposed to the uniqueness of that line for clays, and b) association of sand behavior to the value of the State Parameter (Been & Jefferies 1985), defined with respect to a unique Critical or Steady State Line. The latter alteration has been achieved both implicitly (Jefferies 1993) and explicitly (Manzari & Dafalias 1997), maintaining at the same time simplicity of equations. Parallel attempts to predict the effect of density on sand behavior without direct reference to the State Parameter have resulted in more complex constitutive equations (e.g. Crouch et al. 1994).

All these relatively new models have been proven more or less successful for monotonic loading. Moreover, some of them have been proposed for cyclic loading as well, given that they can predict realistically sand response for a succession of a few load reversals, and a limited number of tests. Nevertheless, our experience with a number of currently available models is that they cannot predict simultaneously some basic aspects of cyclic response, e.g. degradation of shear modulus and increase of damping, as well as liquefaction resistance, with a unique set of parameters.

The constitutive model presented herein was developed with the aim to fill this gap. This capability is demonstrated through one-to-one comparison with typical results from cyclic loading tests, but also through summary comparison with experimental results for a wide range of number of cycles, consolidation stresses and shear stress-strain amplitudes.

2 OUTLINE OF CYCLIC BEHAVIOR

Current state of knowledge asserts that the cyclic behavior of sands is mainly influenced by the amplitude of the cyclic shear strain γ_c (e.g. Ishihara 1982, Dobry & Vucetic 1987, Sagaseta et al. 1991). Hence, for all practical purposes, cyclic sand behavior may be described with reference upon γ_c:

(a) For small values of γ_c ($\leq 5 \times 10^{-4}$ %), the secant shear modulus G_s and the hysteretic damping ratio ξ remain practically constant, equal to the respective initial values G_{max} and ξ_{min}. Regardless of number of cycles, no accumulation of plastic strains or excess pore pressures is observed for this range of γ_c.

(b) For intermediate values of γ_c (5×10^{-4} % $< \gamma_c \leq 10^{-2}$ %), the response becomes non-linear hysteretic. Namely, the secant shear modulus G_s degrades while the hysteretic damping ratio $\xi(\%)$ increases as a function of γ_c (Vucetic & Dobry 1991).
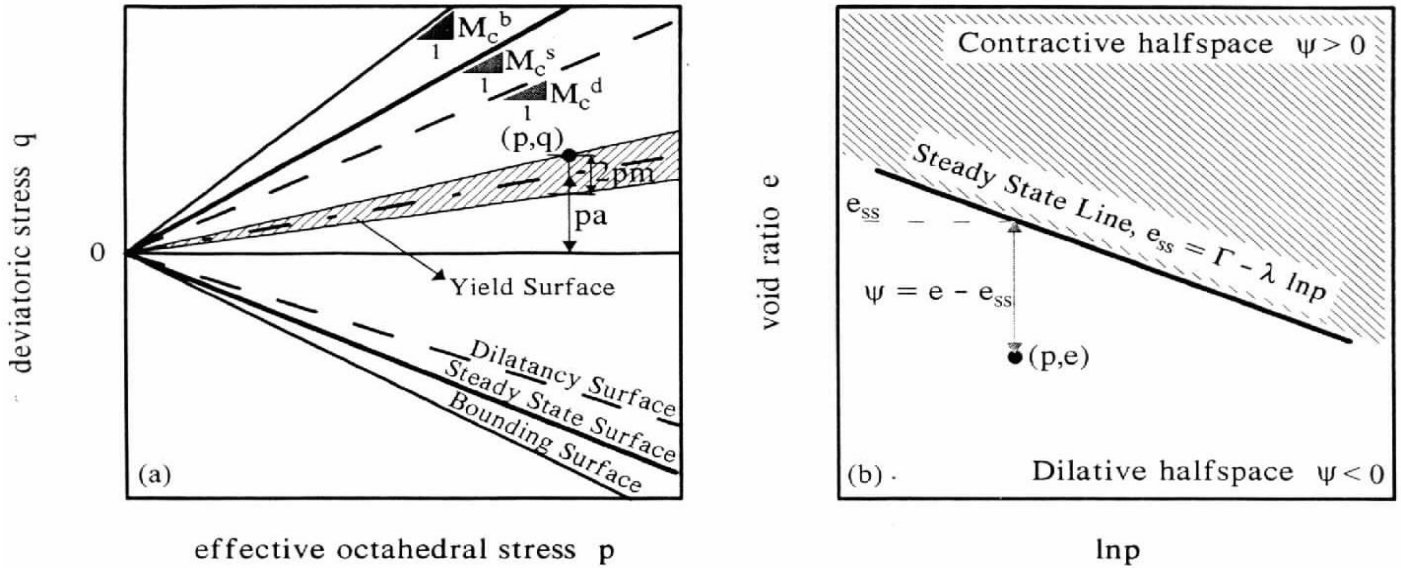
Figure 1. Schematic illustrations of: a) model surfaces in p-q space, and b) Steady State Line in e-lnp space.

Accumulation of plastic strain or excess pore pressure is possible within this range of γ_c, depending on the applied number of loading cycles. However, for earthquake loading, when the number of cycles is relatively small, these effects are not significant and can be readily overlooked (e.g. Vucetic 1994, Ishihara 1996).

(c) For large values of γ_c ($> 10^{-2}$ %), sand behavior becomes clearly elastoplastic. G_s and ξ are very different from their initial values while phenomena of permanent strain accumulation and excess pore pressure build up become dominant. As a result, the number of load cycles plays a key role in describing sand behavior, either in terms of G_s and ξ or in terms of permanent strains and excess pore pressures.

3 PROPOSED FORMULATION

The proposed formulation builds upon the current state of practice for simulating sand behavior, i.e. it uses previously proposed modelling concepts, such as kinematic hardening, two - surface (yield / bounding) plasticity, and the State Parameter ψ in a Critical State Soil Mechanics framework. Specifically, it uses the simple and explicit implementation of ψ introduced by Manzari & Dafalias (1997): ψ is related to the peak stress ratio, an idea initially proposed by Wood et al. 1994, and to the stress ratio at phase transformation, i.e. the state where a dilative sand starts expanding under drained shear (e.g. Ishihara et al. 1975).

Cross-examination of cyclic sand behavior and existing models for sand behavior shows two major inadequacies of the latter: a) the simulation of sand

behavior at small and intermediate shear strains is over-simplified, and b) the effect of sand fabric evolution during loading is essentially overlooked. The proposed model remedies these inadequacies in a CSSM framework by: a) introducing a Ramberg & Osgood (1943) - type of shear behavior within the yield surface, b) relating the size of the yield surface to the threshold cyclic shear strain γ_{tv}, i.e. the limit for permanent strain or excess pore pressure build up during cyclic loading, and c) by introducing a scalar function h_f to account, in a simple way, for the evolution of sand fabric and its effect during cyclic loading.

As a first step, constitutive equations are set in the triaxial stress-strain space (Fig. 1a), which is defined in terms of the effective octahedral and deviatoric stresses: $p = (\sigma_v + 2\,\sigma_h)\,/\,3$, $q = \sigma_v - \sigma_h$ as well as the volumetric and deviatoric strains: $\varepsilon_p = \varepsilon_v + 2\,\varepsilon_h$, $\varepsilon_q = 2\,/\,3\,(\varepsilon_v - \varepsilon_h)$. It is noted that subscripts v and h denote the vertical and horizontal planes respectively.

In this formulation, the Critical or Steady State Line is taken as a known a-priori, unique straight line in the void ratio e - lnp space. According to Been et al. (1991) this is a realistic assumption for sands under stresses that don't cause particle crushing. The State Parameter ψ is defined with respect to the void ratio at Steady State e_{ss} as:

$$\psi = e - e_{ss} = e - \left(\Gamma - \lambda \ln p\right) \qquad (1)$$

To simplify notation, we introduce the deviatoric stress ratio η, as the ratio q/p. The yield surface has a wedge shape in the (p, q) space (Manzari & Dafalias 1997), and is given by:

$$f = \left|\eta - a\right| - m = 0 \qquad (2)$$

where m corresponds to the size of the yield surface and is related internally to γ_{tv} (e.g. Vucetic 1994, Ishihara 1996) as an initial condition (i.e. there is no isotropic hardening), and a is the deviatoric stress ratio that corresponds to the axis of the yield surface. For stress states with f=0, the 'direction' of loading is roughly indexed by s, which is equal to the sign of $(\eta-a)$: s=1 for compression and s=-1 for extension.

Increments of elastic strains are defined in terms of the tangential elastic bulk (K) and shear (G) moduli:

$$K = K_o p_a \left[(1+e)/e \right] \left(p/p_a \right)^b \qquad (3)$$

$$G = \left[G_o p_a \left(p/p_a \right)^b \Big/ \left(0.3 + 0.7e^2 \right) \right] \Big/ a_{ro} \qquad (4)$$

where p_a is the atmospheric pressure in the desired units, G_o, K_o and b are dimensionless model parameters and a_{ro} is the proposed Ramberg-Osgood (R-O)-type formulation:

$$a_{ro} = 1 + w \left(1/a_{ys} - 1 \right) \left(|\eta - \eta_{LR}|/2m \right)^{w-1} \qquad (5a)$$

$$a_{ro} \leq 1 + w \left(1/a_{ys} - 1 \right) \qquad (5b)$$

where η_{LR} is the deviatoric stress ratio at load reversal, and w, a_{ys} are the two dimensionless parameters of the R-O formulation. Based on published experimental data, it may be assumed that a_{ys}=0.8 and w=2 for a wide variety of sands. Equation 5b ensures that for constant p and e, the tangential elastic shear modulus G retains a constant value on the yield surface (f=0).

As portrayed in Figure 1a, the unique Steady State Surface corresponds to a wedge type surface in (p, q) space. This surface is fully described by the line slopes M_c^s and M_e^s that correspond to Steady State reached by loading in compression and extension respectively. Similarly, two more surfaces are being defined in stress space alone: the bounding surface (in terms of M_c^b and M_e^b) and the dilatancy surface (in terms of M_c^d and M_e^d). These surfaces correspond to the deviatoric stress ratio at peak and at phase transformation respectively. Simplifying the proposition of Manzari & Dafalias (1997), all three surfaces are interconnected based on the value of ψ:

$$M_{c,e}^b = M_{c,e}^s + k_{c,e}^b \langle -\psi \rangle \qquad (6a)$$

$$M_{c,e}^d = M_{c,e}^s + k_{c,e}^d \psi \qquad (6b)$$

$$k_e^{b,d} = k_c^{b,d} \left(M_e^s / M_c^s \right) \qquad (6c)$$

where $M_{c,e}^s$ and $k_c^{b,d}$ are four dimensionless model parameters. Symbol <x> is the Macauley bracket

which renders the value of x if x is positive, and zero if x is negative or zero.

The images $M^{s,b,d}$ of the current deviatoric stress ratio η on these three surfaces depend on the 'direction' of loading, and are defined as:

$$M^{s,b,d} = M_c^{s,b,d} \langle s \rangle + M_e^{s,b,d} \langle -s \rangle \qquad (7)$$

Of greatest importance for the formulation is the 'distance' $d^{s,b,d}$ of the current η from these image stress ratios, and the respective total 'size' of these surfaces $d_{ref}^{s,b,d}$:

$$d^{s,b,d} = \left(M^{s,b,d} - s\eta \right) \qquad (8)$$

$$d_{ref}^{s,b,d} = \left(M_c^{s,b,d} + M_e^{s,b,d} \right) \qquad (9)$$

The magnitude of plastic strain increments is a function of the tangential plastic modulus K^p. This is defined as partly governed by the value of the (scalar) fabric evolution function h_f. Namely:

$$K^p = p \left[h_o d^b |d^b| / \| d_{ref}^b - |d^b| \| \right] h_f \qquad (10a)$$

$$h_f = \left[1 + F \langle \int d\varepsilon_p^p \rangle^{t_c} \right] \Big/ \left[1 + F \left(\int \langle -d\varepsilon_p^p \rangle \right)^{t_d} \right] \qquad (10b)$$

where h_o and F are dimensionless model parameters. For soils of the same plasticity index PI, t_c and t_d are more or less constant. For sands, it is appropriate to assume that t_c=2 and t_d=0.75.

Use of the (scalar) fabric evolution function h_f of Equation 10b implies that loading within the dilatancy surface, re-arranges particles to render a 'stiffer' sand (e.g. Ladd et al. 1977, Ishibashi et al. 1988). Moreover, Equation 10b implies that during load reversal from outside the dilatancy surface, sand becomes 'softer' than during loading (e.g. Ishihara et al. 1975). Furthermore, observations suggest that fabric is a function of both the stress and the strain tensor (e.g. Ladd et al. 1977, Ishibashi et al. 1988). Hence, plastic modulus K^p is formulated as a function of both quantities.

Regarding the denominator of Equation 10b sententiously we denote that it is activated only upon load reversal from outside the dilatancy surface. The reason is that its value is proportional to the negative plastic volumetric strain accumulated during the preceded loading, which is non-zero only after a loading path outside the dilatancy surface. Due to length limitations, further details can be found in Papadimitriou (1999).

The ratio of the plastic strain increments is defined as the dilatancy coefficient D. Following the stress-dilatancy theory of Rowe (1962), Manzari & Dafalias (1997) assumed that D is in an arbitrary proportion to d^d.
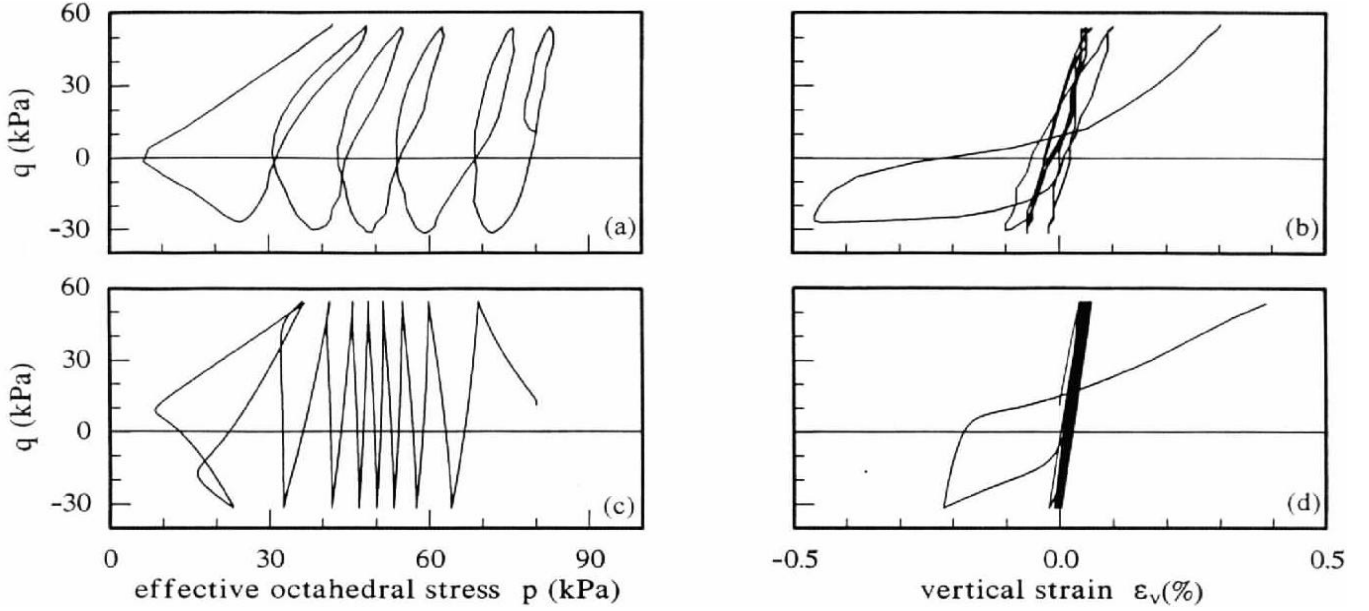
Figure 2. Comparison of measured (a & b) and predicted (c & d) stress path and stress-strain loops for a typical undrained cyclic triaxial test on Nevada sand (D$_r$=60%).

In this model, we maintain this assumption and also introduce dependence on the bounding surface:

$$D = d\epsilon_p^p \big/ \left| d\epsilon_q^p \right| = \sqrt{2/3}\, A_o d^d \big/ \left\| d_{ref}^b - \left| d^b \right| \right\| \quad (11)$$

where A$_o$ is a model parameter, while the square root is introduced for consistency with the generalized 3-D formulation. The denominator in D is only activated upon load reversal from outside the dilatancy surface and aims at predicting what seems as relatively increased increment of volumetric strain.

The plastic shear strain increment is given by:

$$d\epsilon_q^p = s\sqrt{2/3}\langle L \rangle \quad (12a)$$

$$L = sp(d\eta)\big/ K^p \quad (12b)$$

Equations 11 & 12 show that only load paths that cause change in the deviatoric stress ratio η produce plastic strains. Furthermore, the Macauley bracket in Equation 12a allows for merely elastic deformation within the yield surface (f < 0). On the other hand, kinematic hardening of the yield surface ensures stress-strain consistency on the yield surface (f = 0). Specifically:

$$da = s\left[h_o d^b \left| d^b \right| \big/ \left\| d_{ref}^b - \left| d^b \right| \right\| \right] h_f \langle L \rangle \quad (13)$$

In summary, the proposed formulation has a total of twelve (12) positive, dimensionless and density-independent parameters.

4 COMPARISON WITH EXPERIMENTS

The predictive ability of the proposed model is evaluated through comparison with cyclic test data for Nevada sand at 60% relative density and e ≈ 0.65 (Arulmoli et al 1992). Due to length limitations, we concentrate only upon results of resonant column tests (p$_o$ = 40 - 320 kPa) and two-way, nearly symmetric, undrained cyclic triaxial tests (p$_o$ = 40 - 80 kPa). All tests had various amplitudes of cyclic shear stresses and strains. The model parameters used for the predictions are listed below:

Table 1. Values of model parameters

Parameter	Value	Parameter	Value
Γ	0.91	h$_o$	3000
λ	0.022	A$_o$	3
G$_o$	520	M$_c^s$	1.25
K$_o$	160	M$_e^s$	1.25
b	0.5	k$_c^b$	1.80
F	1600	k$_c^d$	1.00

Figure 2 compares predicted to measured stress-strain loops and stress paths during a typical undrained cyclic triaxial test on Nevada sand at 60% relative density. It becomes apparent that the model simulates the experimental measurements reasonably well, with both qualitative and quantitative accuracy. Agreement between measurements and predictions is maintained even upon the triggering of liquefaction, when effective stresses have decreased to a few kPa and shear strains have increased to about 0.4%.
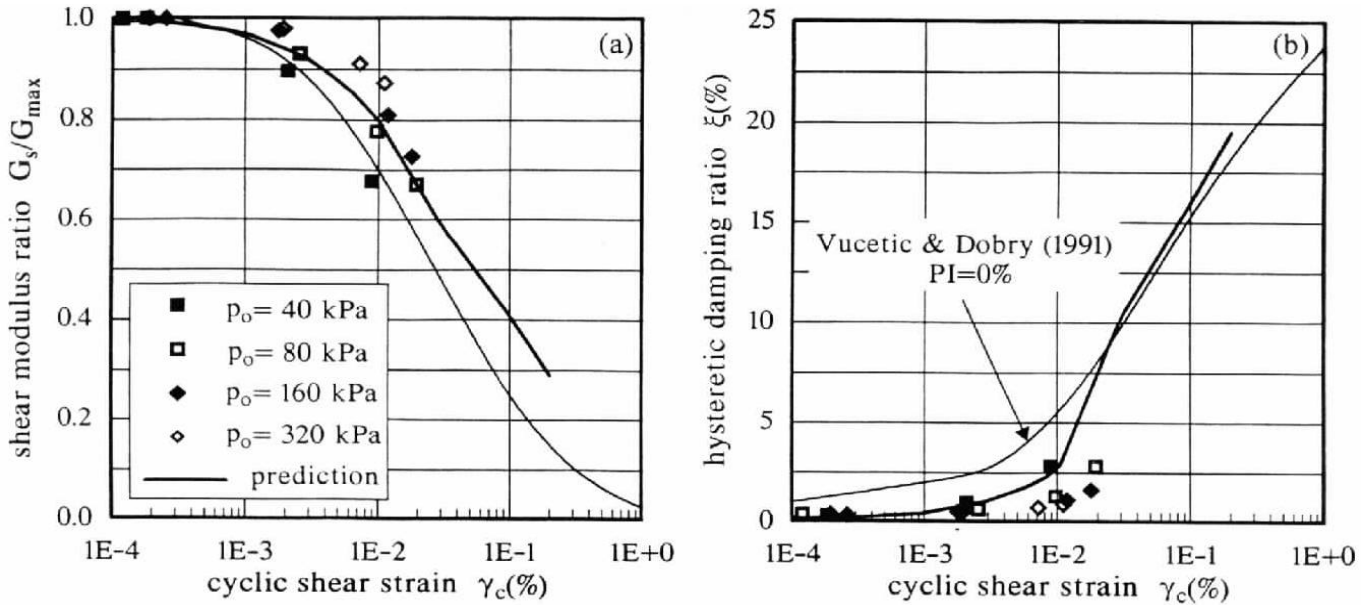
Figure 3. Comparison of measured and predicted values of: a) the shear modulus ratio G_s/G_{max} degradation and b) the hysteretic damping ratio ξ increase with cyclic shear strain γ_c for Nevada sand (D_r=60%).
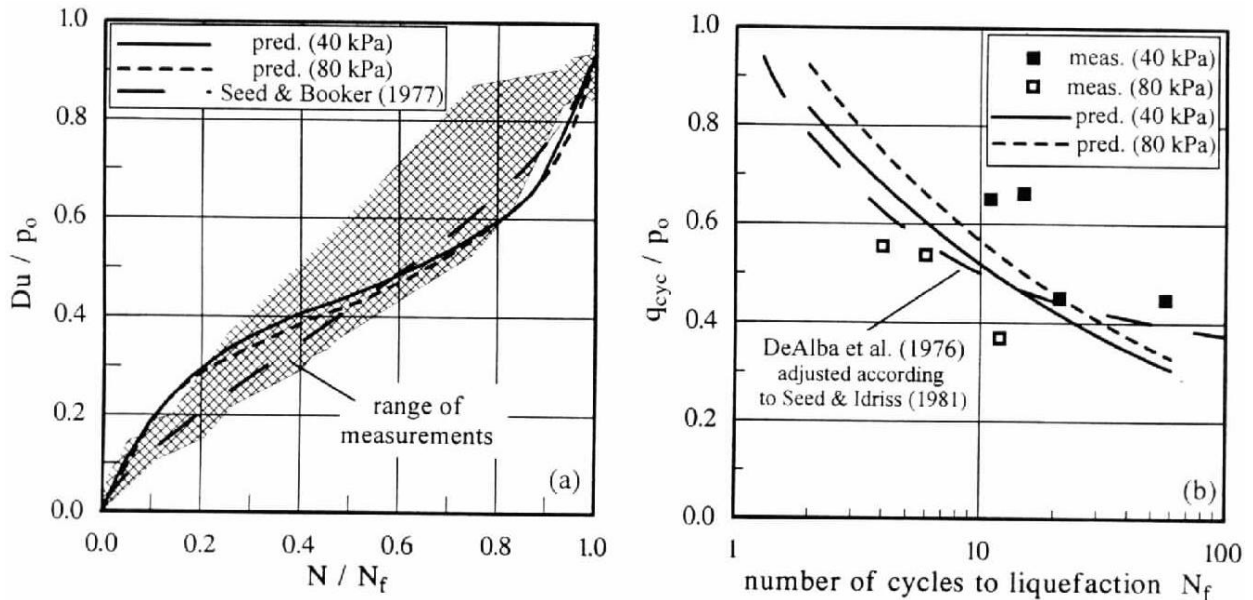
Figure 4. Comparison of measured and predicted values of: a) the evolution of the pore pressure ratio Du/p_o, b) the number of cycles to liquefaction N_f for undrained triaxial loading on Nevada sand (D_r=60%).

In addition to the above detailed comparison, the model is evaluated through summary comparisons which compile results from a number of tests at different stress and strain amplitudes and initial conditions. In this view, Figures 3a & 3b present summary data from the performed resonant column tests for the variation of the shear modulus ratio G_s/G_{max} and the damping ratio ξ with shear strain amplitude. Similarly, Figures 4a and 4b present the summary comparison for undrained cyclic triaxial tests. Namely, Figure 4a refers to the evolution of excess pore pressure ratio Du/p_o with the normalized number of cycles N/N_f, where N_f denotes the number of cycles required for liquefaction, while Figure 4b refers to the variation of number of cycles to liquefaction N_f with the cyclic stress ratio q_{cyc}/p_o.

Each figure compares the analytical predictions to experimental data, as well as to relevant empirical relationships from the literature:

- the relationships for the variation of G_s/G_{max} and ξ for sands proposed by Vucetic & Dobry (1991).
- the relationship proposed by Seed & Booker (1977) for the variation of the excess pore pressure ratio:

$$Du(N)/p_o = (2/\pi)\arcsin\left[\left(N/N_f\right)^{1/1.4}\right] \qquad (14)$$

- the relationship between q_{cyc}/p_o and N_f relationship proposed by DeAlba et al (1976) for simple shear loading and Dr ≈ 60%, corrected according to Seed & Idriss (1981) to account for the triaxial test conditions.

It may be observed that, despite the considerable scatter of the experimental data, analytical predictions provide a reasonable average fit to the test measurements. In addition, they compare well with the trends followed by the more general empirical relationships, which are based on a far larger number of tests on different sands.

5 CONCLUSIONS

An elasto-plastic formulation has been presented which is able to predict both qualitatively and quantitatively the cyclic behavior of a sand for different levels of stress and strain amplitudes, and different consolidation stresses. What is most important is that this is performed with a single set of density-independent parameters and applies to tests with a large number of successive load reversals.

At the present stage of development, the constitutive equations apply strictly to triaxial test conditions. Extension to 3-D stress-strain space is currently under way. This task is necessary for application of the model to other than triaxial test conditions and implementation to numerical codes.

REFERENCES

Arulmoli K., K. K. Muraleetharan, M. M. Hossain & L. S. Fruth 1992. *VELACS: Verification of liquefaction analysis by centrifuge studies - laboratory testing program, soil data report*. The Earth Technology Corporation.

Been K. & M. G. Jefferies 1985. A state parameter for sands. *Geotechnique* 35(2): 99-102.

Been K., M. G. Jefferies & J. Hachey 1991. The critical state of sands. *Geotechnique* 41(3): 365-381.

Crouch R. S., J. P. Wolf & Y. F. Dafalias 1994. Unified critical-state bounding surface plasticity model for soil. *Journ. of Eng. Mech., ASCE* 120(11): 2251-2270.

De Alba P., H. B. Seed & C. K. Chan 1976. Sand liquefaction in large-scale simple shear tests. *Journ. of Geotech. Eng., ASCE* 102(9): 909-927.

Dobry R. & M. Vucetic 1987. State-of-the-art report: Dynamic properties and response of soft clay deposits. *Proceedings, Int. Symp. on Geot. Eng. of Soft Soils, Mexico City.* 2: 51-87.

Ishibashi I., Y.-C. Chen & J. T. Jenkins 1988. Dynamic shear modulus and fabric: part II, stress reversal. *Geotechnique* 38(1): 33-37.

Ishihara K. 1982. Evaluation of soil properties for use in earthquake response analysis. In R. Dingar, G. N. Pande & J. A. Studer (ed.) *Numerical Modelling in Geomechanics*: 237-259.

Ishihara K. 1996. *Soil Behaviour in Earthquake Geotechnics*. Oxford: Clarendon Press.

Ishihara K., F. Tatsuoka & S. Yasuda 1975. Undrained deformation and liquefaction of sand under cyclic stresses. *Soils and Foundations* 15(1): 29-44.

Ladd C. C., R. Foott, K. Ishihara, F. Schlosser & H. G. Poulos 1977. Stress-deformation and strength characteristics. *State-of-the-art report. Proceedings, 9th ICSMFE Tokyo*. 2: 421-494.

Jefferies M. G. 1993. Nor-Sand: a simple critical state model for sand. *Geotechnique* 43(1): 91-103.

Manzari M. T. & Y. F. Dafalias 1997. A critical state two-surface model for sands. *Geotechnique* 47(2): 255-272.

Papadimitriou A. G. 1999. Elastoplastic modelling of monotonic and dynamic response of soils. *Ph. D. Dissertation*, National Technical University of Athens Greece (submitted).

Ramberg W. & W. R. Osgood 1943. Description of stress-strain curve by three parameters. *Techn. Note 902, National Advisory Committee for Aeronautics*. Washington D. C..

Roscoe K. H., A. N. Schofield & C. P. Wroth 1958. On the yielding of soils. *Geotechnique* 8(1): 22-53.

Rowe P. W. 1962. The stress-dilatancy relation for static equilibrium of an assembly of particles in contact. *Proc. of the Royal Society A269*: 500-527.

Sagaseta C., V. Cuellar & M. Pastor 1991. Cyclic Loading. *Proceedings, 10th ECSMFE, Florence.* 3: 981-999.

Seed H. B. & J. R. Booker 1977. Stabilization of potentially liquefiable sand deposits using gravel drains. *Journ. of the Geotech. Eng. Div., ASCE* 103(7).

Seed H. B. & I. M. Idriss 1981. Soil motions and ground liquefaction during earthquakes. *EERC Series*. UC Berkeley.

Schofield A. N. & C. P. Wroth 1968. *Critical state soil mechanics*. McGraw-Hill.

Vucetic M. 1994. Cyclic threshold shear strains in soils. *Journ. of Geotech. Eng., ASCE* 120(12): 2208-2228.

Vucetic M. & R. Dobry 1991. Effect of soil plasticity on cyclic response. *Journ. of Geotech. Eng., ASCE* 117(1): 89-107.

Wood D. M., K. Belkeir & D. F. Liu 1994. Strain softening and state parameter for sand modelling. *Geotechnique* 44(2): 335-339.